

## Review Article

# Potentiostats for Protein Biosensing: Design Considerations and Analysis on Measurement Characteristics

Saad Abdullah , Sarah Tonello , Michela Borghetti , Emilio Sardini ,  
and Mauro Serpelloni 

*Università degli Studi di Brescia, Dipartimento di Ingegneria dell'Informazione, Via Branze 38, 25123 Brescia, Italy*

Correspondence should be addressed to Mauro Serpelloni; [mauro.serpelloni@unibs.it](mailto:mauro.serpelloni@unibs.it)

Received 29 November 2018; Accepted 14 February 2019; Published 17 March 2019

Academic Editor: Bruno C. Janegitz

Copyright © 2019 Saad Abdullah et al. This is an open access article distributed under the Creative Commons Attribution License, which permits unrestricted use, distribution, and reproduction in any medium, provided the original work is properly cited.

The demand for the development of swift, simple, and ultrasensitive biosensors has been increasing after the introduction of innovative approaches such as bioelectronics, nanotechnology, and electrochemistry. The possibility to correlate changes in electrical parameters with the concentration of protein biomarkers in biological samples is appealing to improve sensitivity, reliability, and repeatability of the biochemical assays currently available for protein investigation. Potentiostats are the required instruments to ensure the proper cell conditioning and signal processing in accurate electrochemical biosensing applications. In this light, this review is aimed at analyzing design considerations, electrical specifications, and measurement characteristics of potentiostats, specifically customized for protein detection. This review demonstrates how a proper potentiostat for protein quantification should be able to supply voltages in a range between few mV to few V, with high resolution in terms of readable current (in the order of 100 pA). To ensure a reliable quantification of clinically relevant protein concentrations (>1 ng/mL), the accuracy of the measurement (<1%) is significant and it can be ensured with proper digital-to-analog (10-16 bits) and analog-to-digital (10-24 bits) converters. Furthermore, the miniaturisation of electrochemical systems represents a key step toward portable, real-time, and fast point-of-care applications. This review is meant to serve as a guide for the design of customized potentiostats capable of a more proper and enhanced conditioning of electrochemical biosensors for protein detection.

## 1. Introduction

An increasingly investigated aspect in the research field of pharmaceuticals, biotechnology, and diagnostic is represented by the development of low-cost devices which could give a fast, reliable, noninvasive feedback on physiological and biological processes [1].

Most of the techniques available in biotechnology laboratories for biomolecule investigation are mostly expensive, time-consuming, and highly operator-dependent. Moreover, they are often harmful for the samples and able to give only qualitative or semiquantitative feedbacks rather than sensitive and precise measurements. In this picture, the development of electrochemical sensing devices for the detection and investigation of biomolecules including metabolites, nucleic acids, and proteins plays an important role in medical diagnostics [2–4]. High selectivity, sensitivity,

standardization, and low limit of detection (LOD) represent the key points required in order to compete with the standard biochemical assays. These aspects are primarily influenced by the choice of materials and geometries for biosensor production and of biomolecules and nanomaterials adopted for the biofunctionalization (e.g., aptamers, antibodies, and coated nanoparticles) [5]. However, in addition to those, the electronic circuit for biosensor conditioning, signal acquisition, and transmission contributes strongly in enhancing the performances of the assay [6]. Thus, the possibility to design a circuit able to specifically select the proper electrochemical methods and to enhance the small currents from redox reactions represents a powerful tool to improve the performances of standard biochemical assays [7].

The instrumentation for electrochemical biosensors can be divided in four functional blocks, including signal processing, readout circuit, potentiostat, and signal generator

[8, 9]. Among these, potentiostat represents the core unit of the acquisition system, which significantly influences the sensitivity of the overall measurement [10, 11]. It functions by regulating the potential difference between reference electrode (RE) and working electrode (WE). Additionally, a potentiostat also measures the flow of current between WE and an auxiliary electrode, usually referred to as counter electrode (CE) [12], due to a redox reaction in the biological fluid which induces the movement of charges [13, 14]. As discussed in detail in the literature [15], the use of three electrodes is required to have a precise control of the potential across the working electrode since the reference electrode has a stable and well-known electrode potential and it is used as a point of reference in the electrochemical cell for the potential control and measurement. Despite this common general operating principle, when dealing with biosensing applications, the design of a sensitive and accurate potentiostat is necessarily related to the specific analyte, the electrochemical method, and the overall requirements needed for each specific biosensing application. Primarily, potentiostats are used to detect or measure specific analytes such as metabolites (glucose, cholesterol, and lactate), ions ( $K^+$ ,  $Na^+$ , and  $Ca^{2+}$ ), and metals (zinc, lead) in biological fluids [16–18]. An accurate detection of these metabolites or ions facilitates in the diagnosis and control or treatment of various diseases, for instance, diabetes, acute heart diseases, hypoxia, coronary heart disease, myocardial infarction, and hypertension [19]. Furthermore, another significant target is represented by proteins, due to their fundamental role as a primary link between information processes and replication at the genetic level [20]. Understanding the protein's action may help in investigating the state of different diseases [21]. The ability to detect protein biomarkers when still present in very low concentrations (pg/mL) might represent a powerful tool for early detection and prevention of the onset of various pathologies. In this light, researchers are increasingly exploring the advancement in the design of biosensors with a properly integrated customized conditioning circuit for achieving higher sensitivity, reliability, and standardization of protein quantification.

Figure 1 shows the increasing trend of using potentiostat for biosensing over the course of 18 years; the trend is obtained through Scopus using specific keywords “voltammetry” and “protein detection.”

The specific focus of this review is the analysis of design considerations, electrical specifications, and measurement characteristics of potentiostats specifically customized for protein detection. After a brief overview of the main potentiostat operational modes, a comprehensive and updated review of the most relevant and promising potentiostat designs for protein investigation will be given. In addition, the portability and figure of merit of the potentiostats specifically designed for each category application will be deeply discussed.

*1.1. Potentiostat Operational Modes.* The different techniques available for measuring the response or characterising biosensors possibly addressed to protein investigation can be classified in three main operational modes: voltammetric/

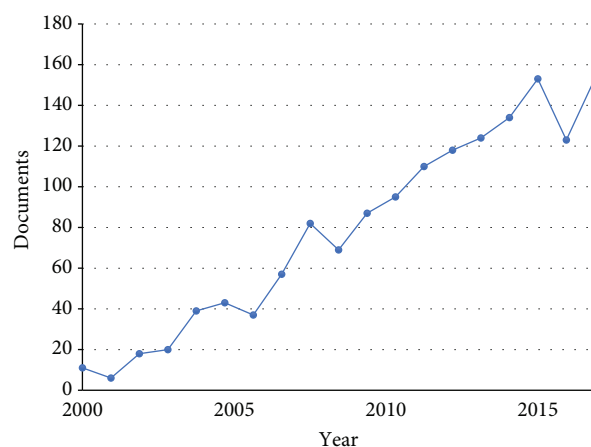


FIGURE 1: Number of documents published on the titled subject over the years.

amperometric, impedimetric and potentiometric, with DC voltages, DC currents, and AC signals as respective responses.

*1.2. Amperometric Protein Detection.* The term “amperometric” comprehends all electrochemical techniques measuring the current as a function of an independent variable that is, typically, time or electrode potential [15]. Thus, subclasses of amperometry are usually considered chronoamperometry (CA), including experiments carried out at fixed electrode potential, and voltammetry, including all the methods that measure a current by varying the potential applied to the electrode [22]. Figure 2 presents the general schematic representation of the amperometric technique. An input signal is applied at OP1 which is a control amplifier and receives a negative feedback from the reference electrode to maintain the output; the working electrode is connected to the transimpedance amplifier which serves as a current-voltage converter. The plot of the output current versus the applied potential is termed as voltammogram as shown in Figure 3. According to the waveform of the potential, the most frequently adopted voltammetric techniques are cyclic voltammetry (CV) (triangular waveform), linear sweep voltammetry (LSV) (ramp), and squarewave voltammetry (SWV) (multistep) [23–25]. Thus, a potentiostat in amperometric mode should be able to control the potential between WE and RE, according to a desired waveform, and detect electrons moved from the electrode to the analyte or from the analyte to the electrode as a current flowing between WE and CE [13, 23, 24]. Thus, current flowing between WE and CE due to analyte reduction/oxidation at metal electrodes will be influenced by the potential applied, by analyte properties, and by its concentration. Among the techniques introduced, CV and LSV are the most commonly used to characterize biosensor active areas and to evaluate the oxidation and reduction processes of proteins by means of direct electrochemistry or enzyme-mediated approaches [25]. The potential-current curve (named voltammogram) obtained in CV and LSV correlates the protein concentration with the height of specific oxidation and/or reduction peaks against the applied voltage [22]. The main issues encountered

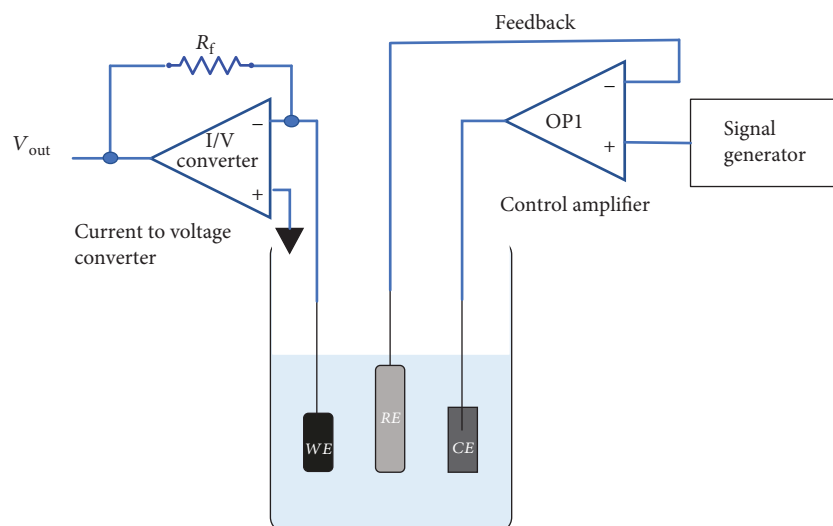


FIGURE 2: Schematic representation of amperometric protein detection where OP1 is a control amplifier.

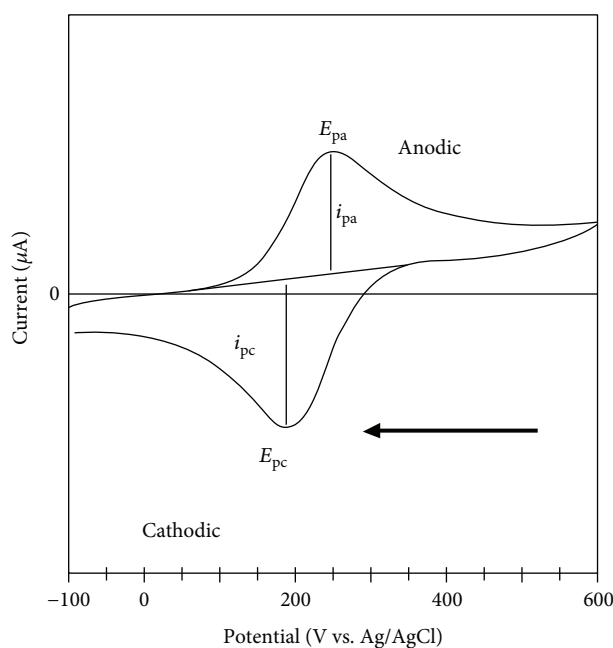


FIGURE 3: Typical voltammogram where  $i_{pa}$  and  $i_{pc}$  represent, respectively, anodic and cathodic peak current,  $E_{pa}$  and  $E_{pc}$  represent, respectively, anodic and cathodic peak current, and  $E_{pc}$  is recreated from [26].

with CV are represented by the high background current and by interfering peaks due to the impurity of the solution used for voltammetry. Also in some cases, there exists DC current noise in the circuits due to improper use of the decoupling capacitor (Figure 3) [26]. Other techniques as SWV and CA are often considered as alternatives to CV. Thanks to the minimal contributions from nonfaradaic currents, SWV is considered to enhance the sensitivity and suppress background currents much more effectively than CV. Furthermore, CA, more often used in enzyme-mediated assays, is considered to give a better signal-to-noise ratio in

comparison to other amperometric techniques [27]. In this light, it emerges that a performing potentiostat should be able to control the potential on the CE with a high accuracy in order to avoid the signal from interfering species and to amplify the current from redox reaction with a high gain, high sensitivity, and reliability, in order to maximize the signal-to-noise ratio and provide reliable calibration curves.

Those aspects have been addressed in terms of potentiostat design considerations in several works, with very different approaches. An interesting portable amperometric electrochemical potentiostat circuit was proposed by Loncaric et al. [28]. The overall setup of the electrochemical cell was designed (Figure 4) in order to ensure the portability of the device. The DAC receives its input from the microcontroller unit and gives its output to the buffering unit, represented by opamp 1 (Figure 5). The peak current measured by the proposed potentiostat differs by  $\pm 5\%$  from the one measured by a conventional benchtop potentiostat. The accuracy of the system could be increased by using an external higher-bit ADC in addition to the current-to-voltage converter. Additionally, the potentiostat includes the operational amplifiers 2 and 3, whereas the circuit of opamp 4 serves as a current-to-voltage converter. Loncaric et al. designed the USB-powered potentiostat circuit which is governed by an Arduino microcontroller (Arduino Duemilanove), able to generate the ramp signal within the range of  $-2.5\text{ V}$  to  $+2.5\text{ V}$  and scan rate of  $10\text{ mV/s}$  to  $50\text{ mV/s}$ . To indicate the initial point of detection, cyclic voltammetry measurements were done at a scan rate of  $500\text{ mV/s}$  with lysozyme concentrations from  $0.5\text{ }\mu\text{g/mL}$  to  $5\text{ }\mu\text{g/mL}$ . The cyclic voltammetry curves reported the stripping voltage  $-0.4\text{ V}$  and cathodic peak  $7.4\text{ nA}$ . The results suggest that this potentiostat can detect even low concentrations ( $0.5\text{ }\mu\text{g/mL}$ ) of the lysozyme, indicating that it performs as well as a standard electrochemical setup.

Another similar example can be found in Muid et al. [29]. Authors designed a low-cost potentiostat by focusing on its conditioning circuit. The schematic of the electrochemical

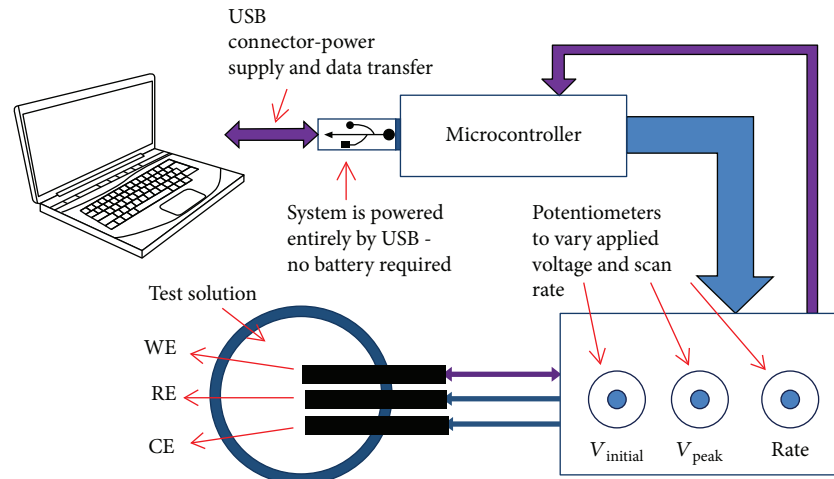


FIGURE 4: Portable design of a USB-powered electrochemical biosensor. Reprinted from [28].

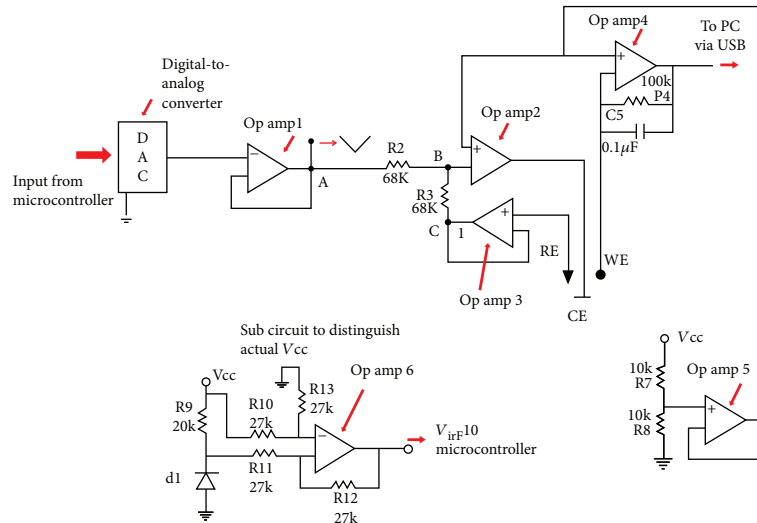


FIGURE 5: Analog circuitry of the potentiostat. Reprinted from [28].

system is similar to [28] but powered by RS-323. This study [29] did not investigate the detection of any particular protein; rather, it is focused on the designing of the potentiostat system (Figure 6). Muid used the ATXmega32 microcontroller, which contains an internal DAC for the generation of waveforms with a sampling rate of 1 Ms/s and an internal ADC with a resolution of 12 bits and sample rate up to 2 MS/s. The analog control circuit for the potentiostat used opamps characterized with small output current and low input impedance. The conditioning circuits amplify the applied voltages ranging from +10.42 mV to -10.42 mV. The output from the DAC is applied to the sample through the analog circuit. At the readout circuit, the measured current is converted into a digital signal through ADC and saved in RAM. The range of the measured potential is  $\pm 1.6$  V at frequencies ranging from 1 Hz to 1 kHz. CV, SWV, and LSV were applied to check the performances of the developed potentiostat, obtaining the minimum error of 0.5%. The

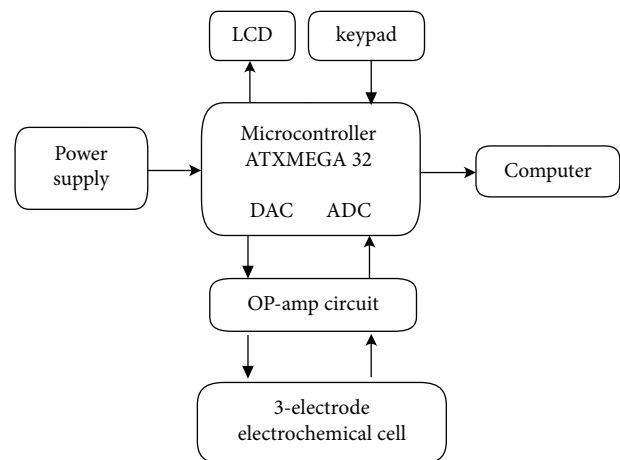


FIGURE 6: Block diagram of the proposed potentiostat. Recreated from [29].

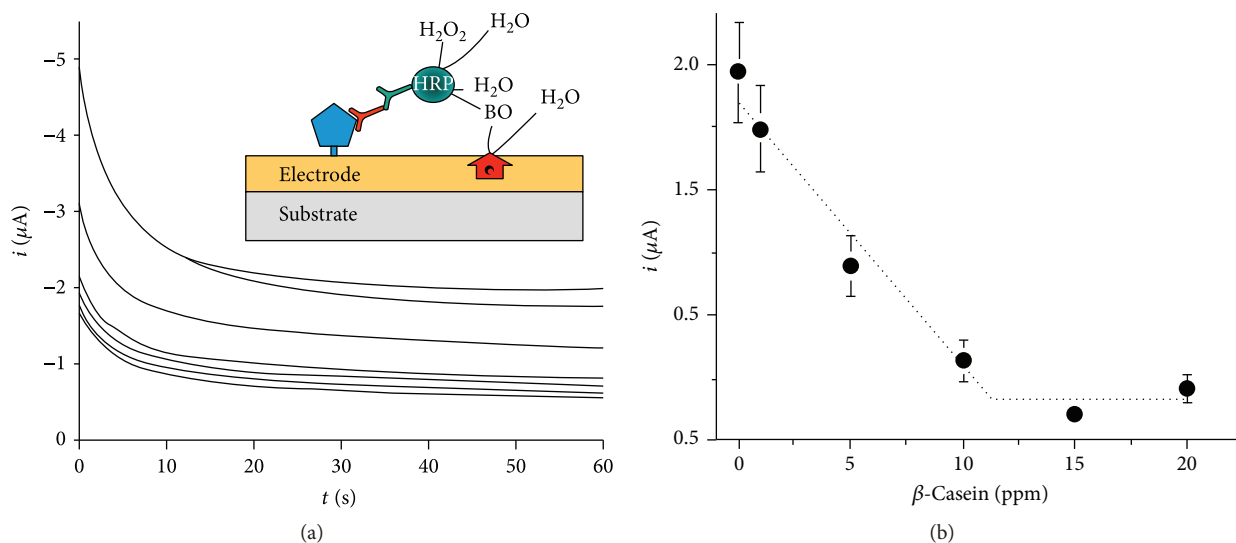


FIGURE 7: (a) Current vs. time curve. (b) Current measurement with respect to  $\beta$ -casein concentration. Reprinted from [32].

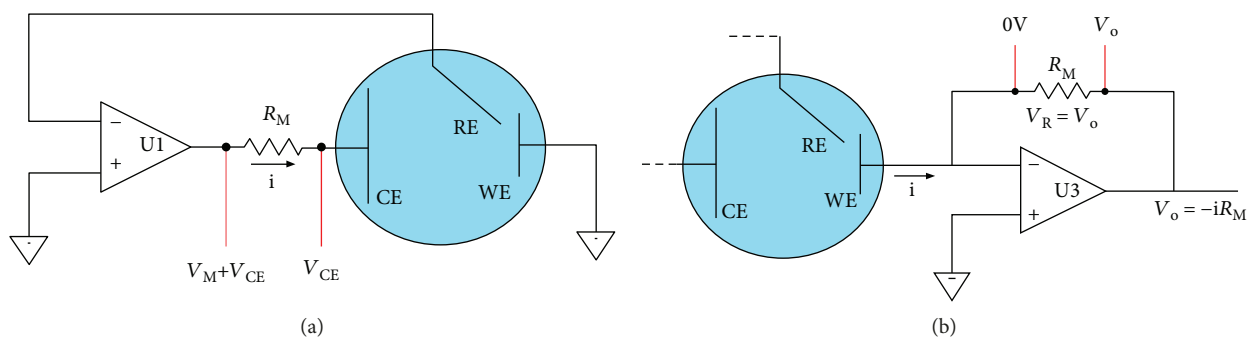


FIGURE 8: Cell I-to-V conversion for ADC. (a) Current measurement through shunt resistance. (b) Current measurement by using a transimpedance amplifier. Reprinted from [33].

overall design and performance of [29] made it eligible to be used for protein biosensing in an amperometric mode.

Similar to [28], Kellner et al. [30], and Kwakye and Baeumner [31], Molinari et al. [32] also investigate the efficiency of a portable immunobiosensor designed for detection of  $\beta$ -casein (food allergen). Since the maximum threshold concentration of allowed allergens in the food is  $10 \text{ mg/L}$ , detection of  $\beta$ -casein was optimised within the range of  $0$ - $10 \text{ mg/L}$ . For the amperometric detection of bonded  $\beta$ -casein, an appropriate redox mediator and hydrogen peroxide are added at an electrode. The voltage of WE was fixed at  $-0.28 \text{ V}$ , and the resulting measured current, inversely proportional to the  $\beta$ -casein concentration (Figure 7(b)), was in the range between  $0.72 \mu\text{A}$  and  $2 \mu\text{A}$ . Its sensitivity, together with portability and Bluetooth connectivity, makes this device appealing in comparison to other commercial methods.

Likewise, Dryden and Wheeler [33] also developed a portable, open-source potentiostat (DStat) specifically for high-performance voltammetric and amperometric measurements in research laboratories. In contrast to commercial potentiostats, its open nature, adaptation to experiments, and modifiable operations make it more attractive. The

potentiostat is powered and controlled via a USB connection allowing portability. Though the ATxmega256A3U microcontroller has an in-built 12-bit DAC, an external 16-bit DAC is employed to reduce the quantization error. DStat measures the current by means of a transimpedance amplifier circuit in series with the WE (Figure 8(b)) rather than using a shunt resistor  $R_M$  (Figure 8(a)). The conversion of the WE electrode current into voltage is performed by a 24-bit ADC. The microcontroller updates the DAC, collects data from 24-bit ADC, and sends them to a computer for analysis and storage. To test the performance of the potentiostat,  $10 \text{ mM}$  potassium hexacyanoferrate(III) and 4-aminophenol solutions were used. As presented in Figure 9, DStat gave smooth responses without noise distortion for potassium hexacyanoferrate(III) measurements in contrast to other commercial potentiostats. Moreover, differential pulse voltammetry measurements (Figure 9(b)) depicted the capability of DStat to measure low-output currents. Being an open-source potentiostat, the electronic hardware and software both are completely accessible, improving the flexibility and scope of usage.

Sun et al. [34] designed a multifunctional reconfigurable electrochemical cell that can be toggled between

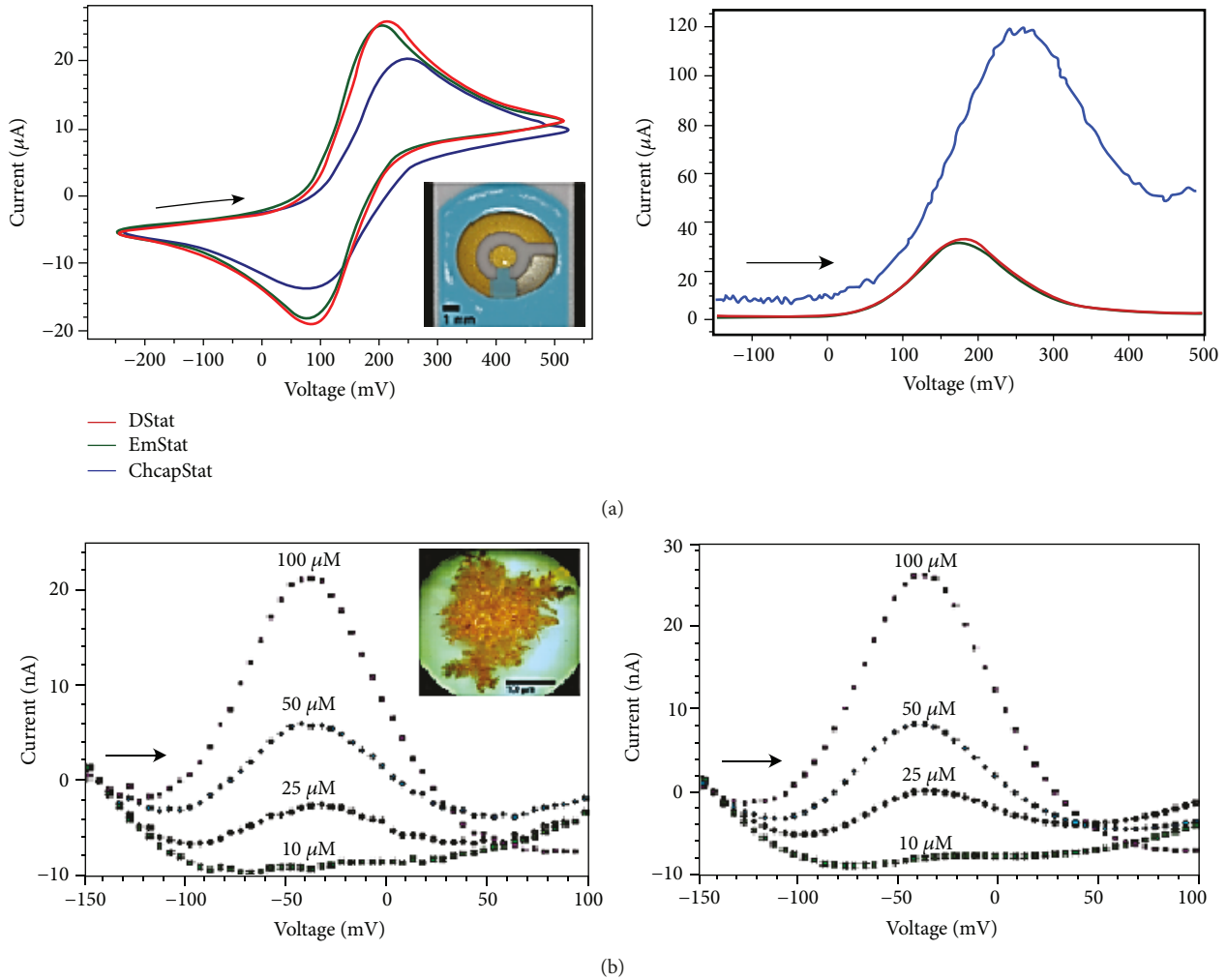


FIGURE 9: Voltammetric measurement comparison. (a) Cyclic voltammetry (left) and squarewave voltammetry (right) of potassium hexacyanoferrate (III). (b) Differential pulse voltammetry of 4-aminophenol, DStat (left), and EmStat (right). Reprinted from [33].

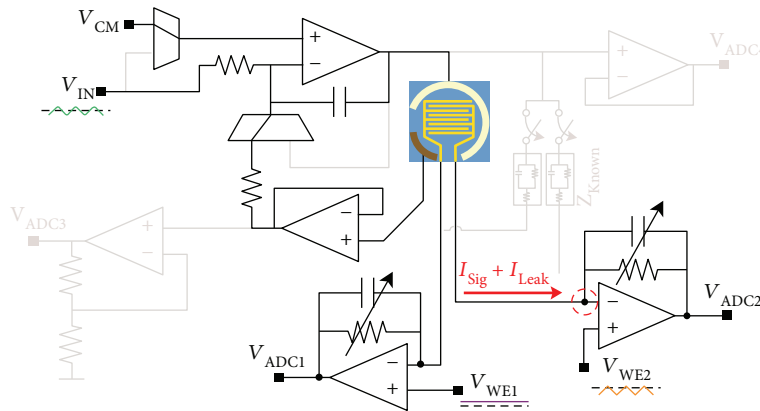


FIGURE 10: Schematic of potentiostat in amperometric mode. Reprinted from [34].

amperometric, potentiometric, and impedimetric modes. The general components of the potentiostat are the same, including 14-bit DAC and 16-bit ADC (Figure 10). Focusing on the amperometric mode, the evaluation was performed by using lactoferrin as the target molecule.

The application of  $-0.2\text{ V}$  to  $0.3\text{ V}$  with the  $25\text{ mV/s}$  scan rate can detect LTF in biological fluids. The measurement range of this potentiostat is  $\pm 1\text{ nA}$  to  $\pm 200\text{ }\mu\text{A}$ , and the approximate resultant current of this test ranges from  $40\text{ }\mu\text{A}$  to  $150\text{ }\mu\text{A}$ .

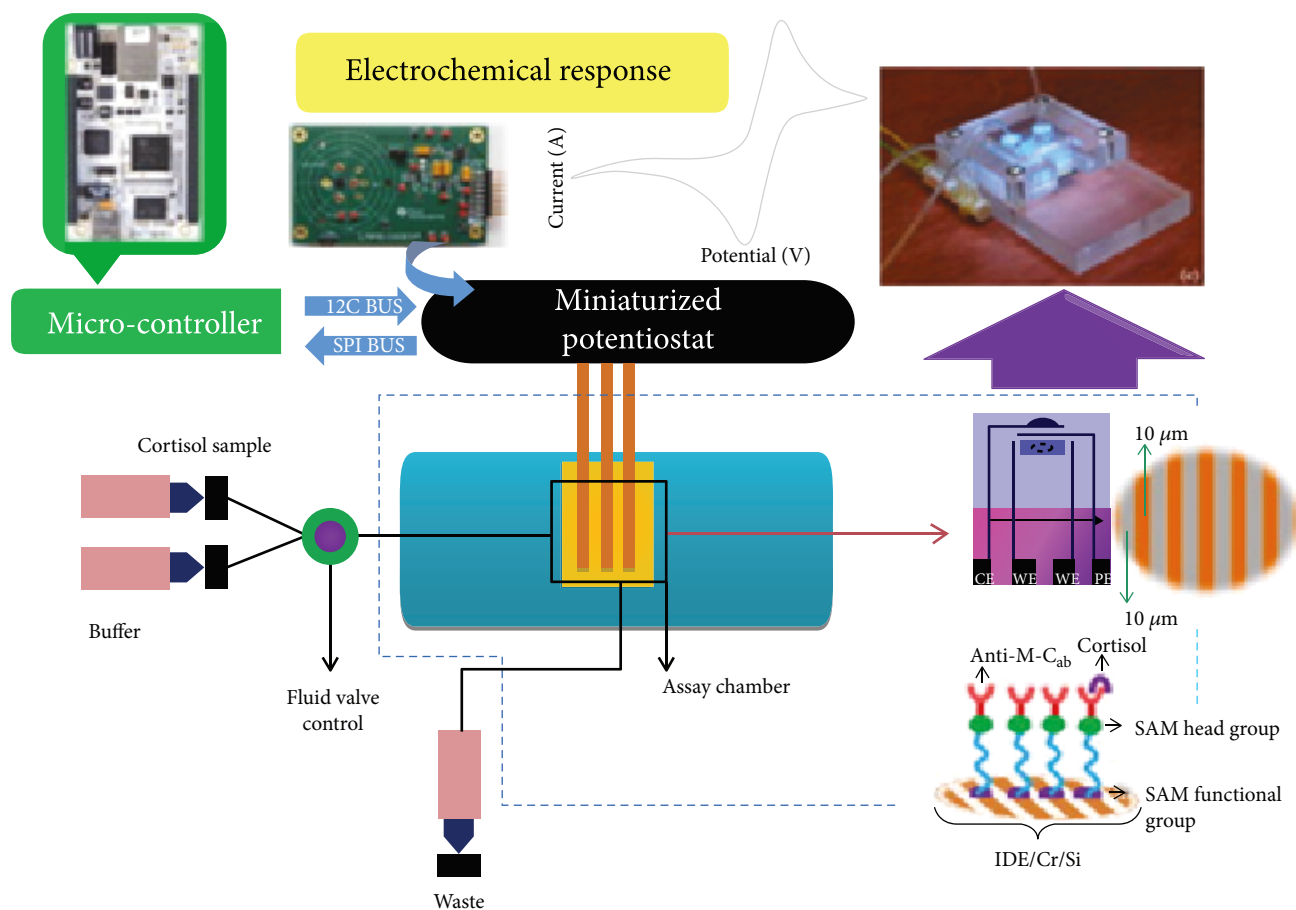


FIGURE 11: Miniaturized potentiostat-based system for cortisol detection. Reprinted from [19].

For the detection of biomarkers through the voltammetric technique, Cruz et al. [19] used a novel approach to design a potentiostat by using a miniaturized chip LMP91000. The readout circuit measures the current at the output stage via a transimpedance amplifier and converts it into a proportional voltage. This acquisition of the potentiostat signal is transmitted to the built-in ADC161S626 (16-bit), embedded on the LMP chip (Figure 11). The potentiostat exhibits low detection limit and high sensitivity for cortisol detection, suggesting that this can be used for detection of other biomarkers at point of care (POC).

Ghoreishizadeh et al. [35], Ainla et al. [36], Giordano et al. [37], and Steinberg et al. [38] developed a wireless method of data acquisition and support miniaturisation of the biosensing platform by designing an amperometric potentiostat with a readout circuit to measure the differential current. Ghoreishizadeh et al. [35] used an off-chip microcontroller which generates different profile voltages for the excitation of the potentiostat by means of a 10-bit DAC (Figure 12). The output received at WE goes through a programmable gain amplifier to reach a 10-bit ADC. The maximum measurable output current of this potentiostat is  $20 \mu\text{A}$ , whereas the minimum detectable change is  $0.47 \text{ pA}$ .

Medina-Sánchez et al. [39] used on-chip magnetic beads as a preconcentration platform and linked it with the quantum dots for efficient and sensitive detection of

apolipoprotein E (ApoE). The technology used for electrochemical detection of ApoE is SWV. The results showed a stripping peak at  $-0.85 \text{ V}$  with frequency  $25 \text{ Hz}$  and  $0.11 \mu\text{A}$  current (Figure 13). The potentiostat detects the ApoE protein linearly from  $10 \text{ ng mL}^{-1}$  to  $200 \text{ ng mL}^{-1}$  concentrations.

From a critical evaluation of the research papers presented, it appears clearly that measurement performance of the potentiostat is mainly affected by the selection of opamps. In response to the applied voltage, the biosensing system produces a small amount of current, thus requiring an opamp with low-input bias currents. Afterwards, this resultant signal serves as the input to the ADC; hence, amplification of the signal must be ensured to make the current on order of microamperes producing a full-scale signal on the ADC. Enzyme-based amperometric biosensors are subjected to reduction in signal due to interference from chemicals in the sample.

**1.3. Impedimetric Protein Detection.** In impedimetric mode, a biosensor detects the change in resistance and/or capacitance that occurs during detection events [40, 41]. At equilibrium, the electrolyte-electrode's electrical impedance (AC) is measured by these biosensors. In addition, an impedimetric mode is obtained by applying a sinusoidal stimulus current/voltage with a frequency that varies over time and thus by measuring the resultant voltage/current, whose

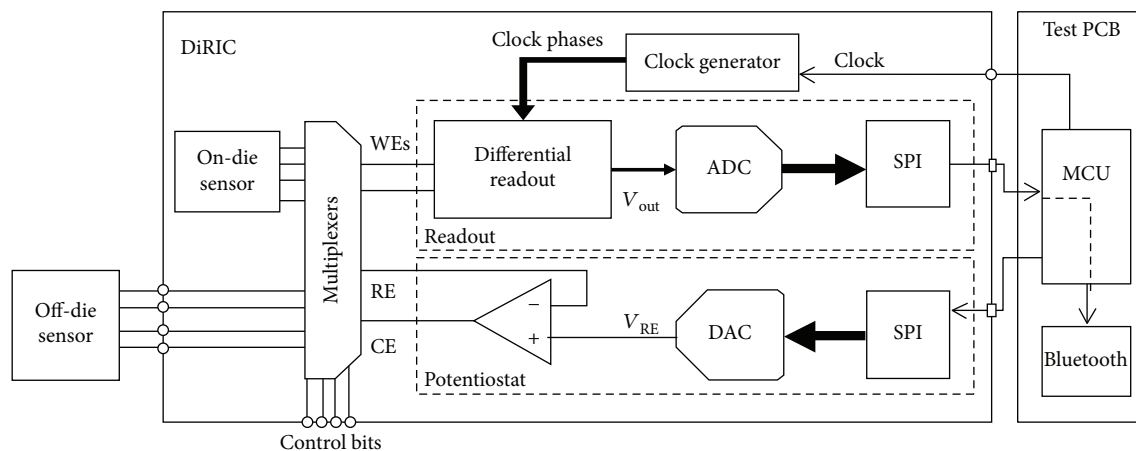


FIGURE 12: Block diagram of a differential readout circuit (DiRIC). Reprinted from [35].

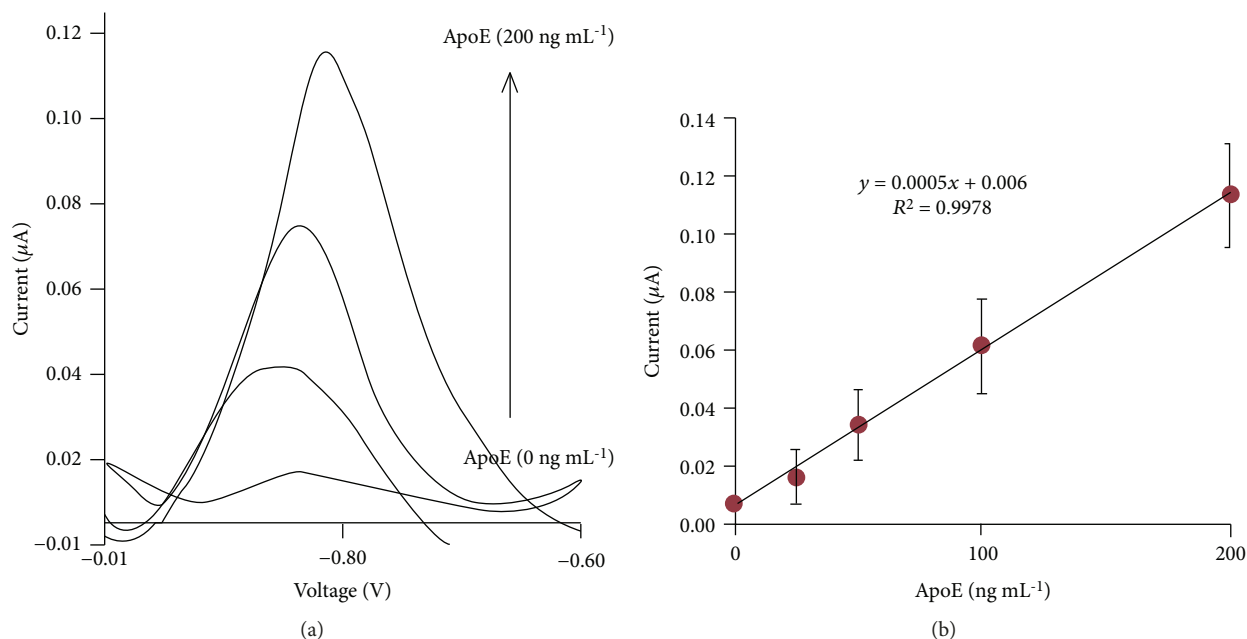


FIGURE 13: (a) Apo-E magnetoimmunoassay performance. (b) Calibration curve of ApoE. Reprinted from [39].

amplitude and phase change provide information related to target molecules. Figure 14 shows the block diagram representation of impedimetric mode for protein detection. A sinusoidal input is generated at CE from a variable frequency generator with an exciting signal within the range of 10 mV; this signal passes through the biosensor chip containing the protein sample, and the resulting signal is acquired by a frequency analyzer/impedance measurement device [42]. This technology is commonly regarded as electrochemical impedance spectroscopy (EIS), most frequently used for monitoring cell cultures but also applicable to the detection of molecules [43], proteins, and enzymes [44]. In EIS, the impedance behaviour of the investigated solution can be described by the combination of the capacitance, the ohmic resistance, the constant-phase element, and the Warburg impedance. When the electrodes are in contact with an

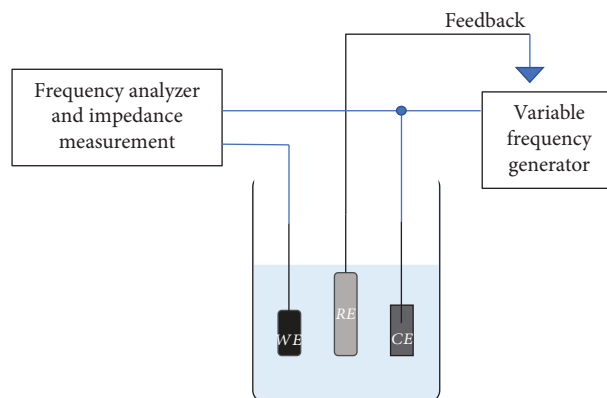


FIGURE 14: Block diagram representation of impedimetric protein detection.

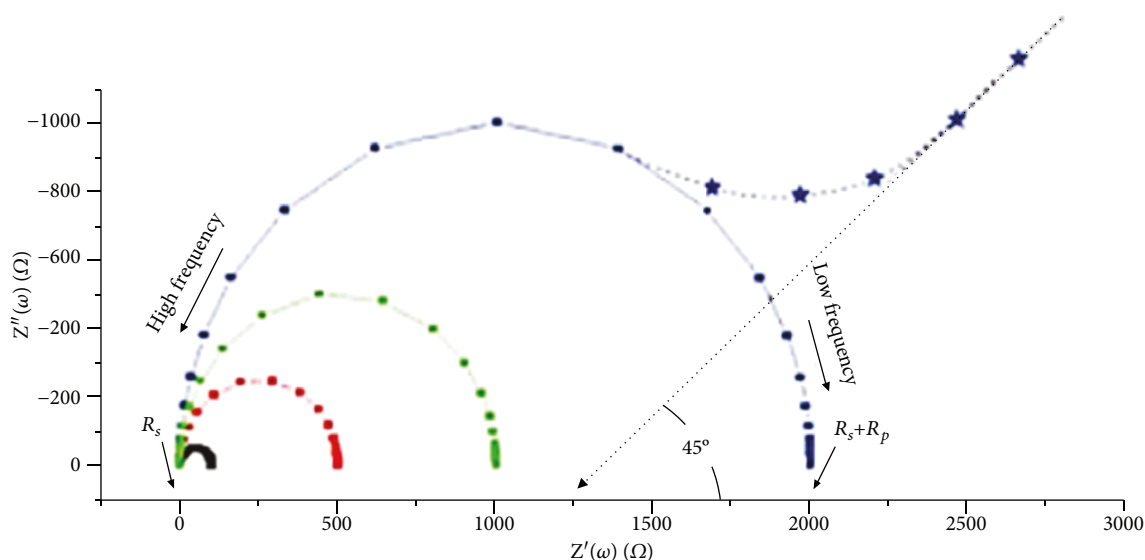


FIGURE 15: Typical Nyquist plot. Reprinted from [45].

electrolyte, the impedance can be modelled by the Randles circuit, which consists of the solution resistance in series with the parallel combination of the double-layer capacitance and the charge transfer resistance in series with the Warburg impedance [42]. In impedimetric mode, impedance data are obtained at the output, and the Nyquist plot is the most conventional way of representing these data. In a Nyquist plot (Figure 15), the imaginary part  $Z''(\omega)$  is plotted against the real part  $Z'(\omega)$  to provide all the vital information related to electrode-electrolyte interference [45].

In contrast to amperometric and potentiometric biosensors, a significant benefit of impedimetric biosensors is represented by the small stimulus voltage (generally 5 to 10 mV) which does not disturb or damage the biorecognition layers. Additionally, the label-free nature of impedimetric biosensors provides measurements without the intervention of label molecules, simplifying the functionalization process [46, 47]. Impedance-based assays rely on the principle that when a biomolecule of interest interacts with the sensing surface, electrical properties of the surface changes as a result of the sole presence of the biomolecule of interest [48]. For this purpose, impedance biosensors are considered advantageous for detection of proteins, reducing the variability introduced by the multiple binding events in label-based assays [46]. However, when a strong selectivity is required, for example when multiple biomarkers need to be discriminated in the same solution, impedance-based detection shows limitations [45], since it is not intrinsically able to discriminate the increase in impedance due to different protein species.

In this light, an impedimetric potentiostat aiming at improving sensitivity should ensure (1) the possibility to easily customize input frequency, (2) very high sensitivity to impedance changes, and (3) finally a proper compensation system to avoid drifting or instrumentation interference with the small changes introduced by biomolecules.

An innovative multifunctional miniature sensing system was designed by Pruna et al. [49] that allows the user to

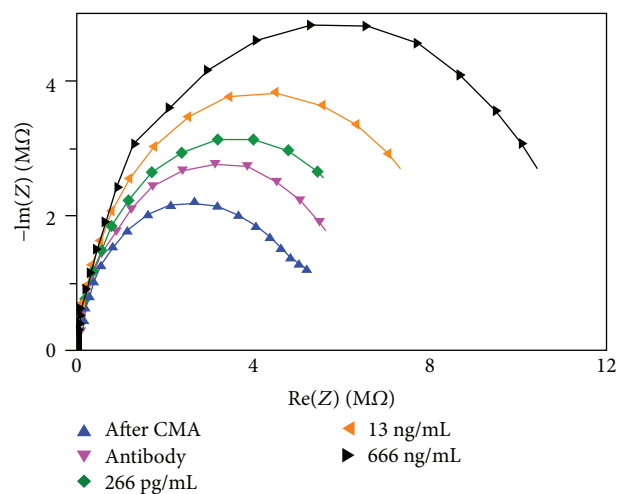


FIGURE 16: Nyquist plot for TNF- $\alpha$  detection at different concentrations. Reprinted from [49].

choose between impedimetric, amperometric, and voltammetric measurements. Two microcontrollers, PIC32 and PIC24, are used for waveform generation, data acquisition, and computer interface. Among these, PIC24 has a 16-bit ADC for data acquisition in biosensing applications in contrast to the 10-bit ADC of PIC32, whereas PIC24 has a 10-bit DAC also. Pruna tested the device for detection of TNF- $\alpha$  at several concentrations (266 pg/mL to 666 ng/mL) with application of excitation voltage  $\pm 2.5$  V and frequency 1-10 kHz. Results are obtained between 1 and 10 Hz where maximum impedance variation can be detected (Figure 16).

Since the full impedance spectrum is a time-consuming technique, Huang et al. [50] employed a potential step-based time domain impedance measurement. All the operational amplifiers in the potentiostat have a bandwidth greater than 1 MHz. The I/V converter amplifier (AD8606) is the

most demanding part of the potentiostat having gain in hundreds. Huang used the C8051F060 microcontroller, which has two in-built 16-bit ADCs, two 12-bit DACs, and a voltage reference. Experiments were carried out with *E. coli*, and impedance spectra were obtained by the potential step (STP) method and frequency response analyzer (FRA) method for comparison. For STP, the applied voltage is 10 mV in amplitude, 0.1 second in duration, with a 200 kS/s sampling rate, whereas FRA used the 5 mV AC potential. The impedance spectra acquired by both STP and FRA (Figures 17 and 18) demonstrate precise measurement due to the higher sampling rate. Comparison of the Nyquist diagrams suggests that the potential step-based impedance measurement technique is possible by using a low-cost portable instrument.

For EIS measurements, Ogurtsov et al. [51] designed a two-channel EIS system, consisting of a 16-bit DAC, signal generators, low-pass filters, instrumentation amplifiers, I/V converters, and the ATxmega128A1U microcontroller. For validation of the system, EIS measurements were conducted to measure the T-2 toxin concentration, over a frequency range of 10 Hz to 100 kHz, with an applied potential of 10 mV AC amplitude. The output voltage is amplified and demodulated in the I/Q demodulator to give imaginary and real impedance components. Performed calibration within the range 0-225 ppm showed that the developed biosensor could detect T2 toxin concentrations at the levels below 25 ppm. In impedimetric mode, the potentiostat proposed by Sun et al. [34] measured NeutrAvidin, a type of protein, by using the EIS method. Small sinusoidal voltages (0.2 V) were applied with a variable frequency of 1 Hz-10 kHz. The Nyquist plot (Figures 19 and 20) showed that the resultant impedance ranges from 50 M $\Omega$  to 10 M $\Omega$ , demonstrating that this potentiostat can be used as a label-free biosensor.

In addition to customized research potentiostats, several commercially designed potentiostats can also be found in the literature. Esfandyarpour et al. [52, 53] claimed to have designed an ultrasensitive biosensor that overcame the problem of current limitations by using the VersaSTAT3 potentiostat measuring biomolecular binding in real time. In addition, Bellagambi et al. [54] and Baraket et al. [55] used the VMP3 potentiostat to perform EIS measurement of multiple biomarkers, investigating the selectivity and sensitivity of the device. The Nyquist plots demonstrate that impedance increases with a number of incubations due to adsorption and detection.

From the critical analysis of impedimetric potentiostat design, it arises that the main concerns are related to adequate bandwidth, drifting, and capability to identify phase changes between the applied voltage and the measured current. EIS circuitry requires a high enough bandwidth to detect the small currents at the output. However, higher frequencies are less affected by noise and drift inherent in the measurement electronics while several investigators reported impedance drift at frequencies of approximately 100 Hz and lower [45]. Moreover, any phase error introduced due to measurement circuit must be adjusted to ensure that the input signal is aligned with the output.

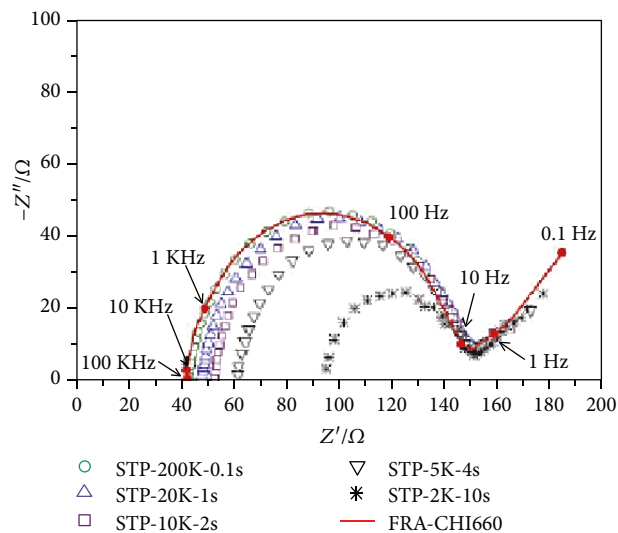


FIGURE 17: Impedance spectra obtained by the STP method with varied sampling rates and the FRA method (red line). Reprinted from [50].

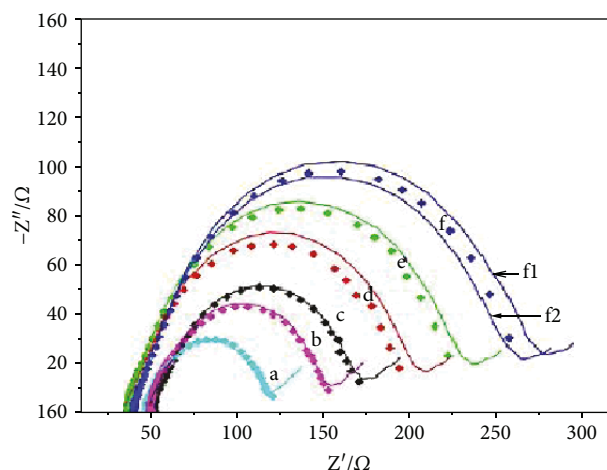


FIGURE 18: Nyquist plots acquired by the STP method (solid diamond) and FRA method (solid line) (a), after epoxy silane modification, (b) after antibody attachment, (c) and after *E. coli* cells bonding with cell concentration of  $1 \times 10^5$  cfu/mL, (d)  $1 \times 10^6$  cfu/mL (e), and  $1 \times 10^7$  cfu/mL. (f) In the f data set, f1 and f2 denote that they are measured before and after STP measurement. Reprinted from [50].

**1.4. Potentiometric Protein Detection.** In potentiostatic or potentiometric mode, the potentiostat measures the voltage difference between WE and RE in the absence of current flow between the electrodes, while controlling the potential of CE with respect to WE (Figure 21). The resulting potential difference depends on the concentration of an analyte [13, 23]. Some potentiometric biosensors are known as redox-potential biosensors due to the involvement of redox reactions. In all cases, the potentiometric response is determined by ion conduction processes and ion exchange reactions at

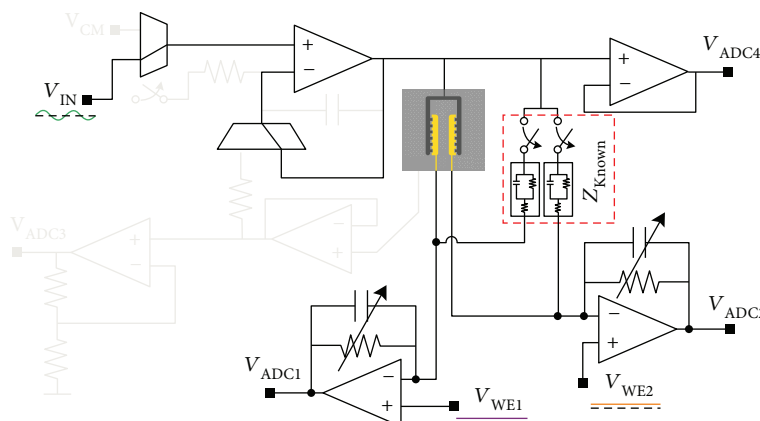


FIGURE 19: Schematic of potentiostat in impedimetric mode. Reprinted from [34].

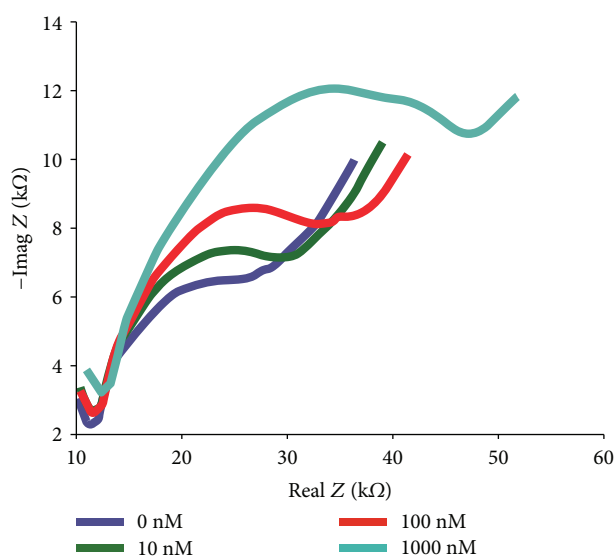


FIGURE 20: Nyquist plot for NeutrAvidin. Reprinted from [34].

the solution interface/membrane. Potentiometric biosensors can detect free ions and need frequent calibration.

From an analysis of the works addressing the design of potentiometric potentiostats in the recent literature, the main concerns are the input impedance and input bias current. The input impedance of such biosensors is very high, usually on the order of  $100\text{ M}\Omega$ , which demands high-resolution sampling of the electrode voltage usually in the range of 12 bits to 24 bits. A voltage follower circuit is generally used to (1) provide a high impedance interface, so the output signal can be isolated from the source signal effectively. In addition, the instrumentation amplifier is characterized by high noise elimination capability and the high common mode rejection ratio (CMRR) which is generally  $>80\text{ dB}$  [56]. Potentiometry requires the input bias of the measurement circuit to be very low to reduce the measurement error to less than 1%.

DStat potentiostat [33], in addition to its uses for amperometric applications, is also compatible with voltage-measurement application, such as potentiometry for both

pH and protein detection. In pertinent literature, only one of the lab-built systems had this capability; thus, it makes DStat for potentiometry attractive. Measurements of standard pH calibrations were recorded and compared with the results acquired from an AR50 Benchtop pH meter to evaluate the potentiometric capabilities of DStat. The results of both the instruments were virtually similar as both exhibited the anticipated Nernstian response having a root mean square deviation from  $2.3\text{ mV}$  and  $1.9\text{ mV}$  for DStat and Benchtop, respectively. The higher sample rate of the DStat ( $30\text{ kHz}$  with respect to  $1\text{ Hz}$  of AR50) ensures good temporal resolution.

Moreover, Huang et al. [57] also proposed a potentiometric setup, similar to [58], but with a remote data transmission based on the GPRS communication system. The complete circuitry of the potentiostat consists of the conventional components: a DAC (12-bit), two ADC (12-bit), a microprocessor (AT89C51), a I/V converter, a low-pass filter, a voltage amplifier, and an RS-323 interface (Figure 22). The programmable voltage ranges from  $0$  to  $5\text{ V}$  with a resolution of  $1\text{ mV}$ , while the range of measured current lies between  $1\text{ }\mu\text{A}$  and  $1\text{ mA}$ . The microprocessor is responsible for the source/excitation signal, data acquisition, and configuration management. ADC-1 measures the potential difference between working electrode and reference electrode. A voltage follower is connected to the ADC-1 to avoid loading effect. Based on the ADC-1 output, the microprocessor generates the corresponding control voltage to DAC. Hence, DAC produces a bias voltage to regulate the current injection into CE. In this feedback process, I/V measures the current of the biosensor between WE and CE through a resistor. To evaluate the function of the proposed potentiostat, the pH variation of a solution is measured and compared with a commercial potentiostat. The results acquired from the homemade potentiostat deviated by  $1.82\%$ , with respect to the ones from the commercial potentiostat, and this deviation could be considered negligible in several applications.

Similarly, Sun et al. [34] proposed a portable potentiostat (Figure 23), generalized for various proteins and other biomolecules, which can be integrated into wearable devices and smartphones. As mentioned earlier in Section 1.2, it is a reconfigurable device and can be converted into the

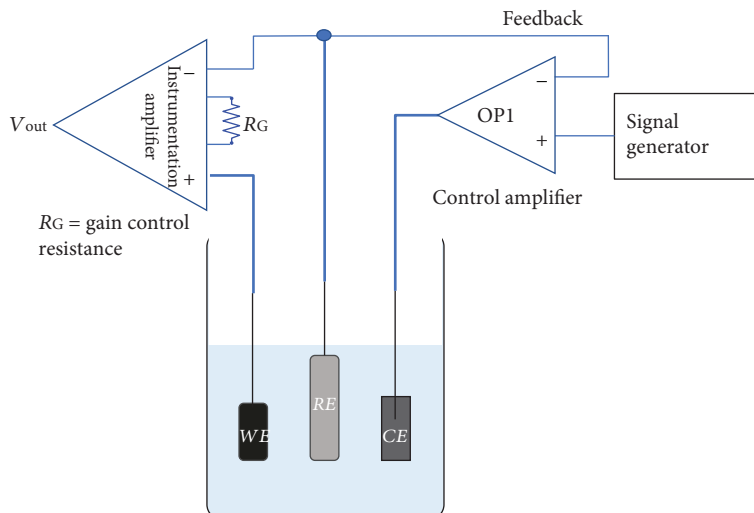


FIGURE 21: Schematic representation of potentiometric protein detection, where OP1 is the control amplifier.

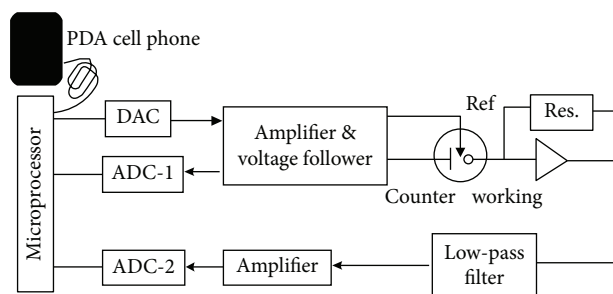


FIGURE 22: Mechanism of the portable potentiostat. Recreated from [57].

potentiometric mode by repurposing the electrical components. The results of pH testing deviated only by 1.2% from the results of a standard test.

Similarly to the previously described works, a potentiometric based on the design for biomolecule analysis, including proteins, is proposed by Ma et al. [59]. Battery-driven, low cost, portability, high performance, and low-power consumption are some of the significant features of the designed potentiostat. The potential difference or open-circuit potential obtained from the electrodes went through amplification followed by filtration. Subsequently, the acquired analog signals were converted via a 12-bit ADC, so they can be transmitted to a PC by passing through MCU (MSP430f149) (Figure 24). The electrochemical analysis was performed to measure the urea concentration. The input potential ranges from  $-0.2$  to  $1$  V, whereas the output voltage ranges from  $0.06$  to  $9.11$  V. The potential at the readout circuit increases as the urea concentration increases, proving the efficiency of the biosensor.

Potentiometric biosensors most often use indicator electrodes that are selectively sensitive to the target molecule, so the recorded potential depends on the activity of the target molecule. The time taken by the electrode to reach equilibrium with the solution affects the accuracy of sensitivity of the measurement because of the presence of interfering ions.

Indeed, most of the electrodes use Ag/AgCl which results in free  $\text{Cl}^-$  ions in the solution hence reducing the sensitivity of the biosensor. Several advancements have been performed to fabricate miniaturized reference electrodes for potentiometric biosensors, but their use is limited due to inadequate stability and reduced lifetime in high ionic strength biological samples [60].

## 2. Discussion and Comparison of Potentiostats

Tables 1–3 summarize the main electrical features and design considerations of different potentiostats used for detection of proteins. For each potentiostat, the tables show bibliography references, specific protein detected, peak voltages and currents, frequency, portability, programmability, and sensitivity. It can be observed from the column of publication year that majority of the studies related to detection of a specific protein with the help of potentiostats have been conducted in the last five years. This shows that research focused on potentiostats for protein detection has become a point of interest over the recent years. Furthermore, the ever-growing demand for fast and reliable medical diagnosis has led to growing interest in electrochemical biosensors, in particular for the quantification of disease-related protein biomarkers for highly investigated pathologies (e.g., cancer, neurodegenerative diseases) in concentration ranges below ng/ml [61, 62].

If we compare the discussed potentiostats in terms of operating voltages, the required voltages fall into two major ranges ( $\pm 0.1$  V and  $\pm 2.5$  V). Thus, it is important to highlight that the variation of operating voltages is typically between  $0.1$  and  $2$  V for the protein detection, in order to avoid any risk of denaturation induced on the protein conformation. In this light, we can observe that the highest accuracy has been obtained in [19] and the highest possibility of customization in [33] which also discusses several design considerations and optimum electronic component selection for higher accuracy. Most of the reported potentiostat units use 12/16-bit DAC to generate the accurate output waveform

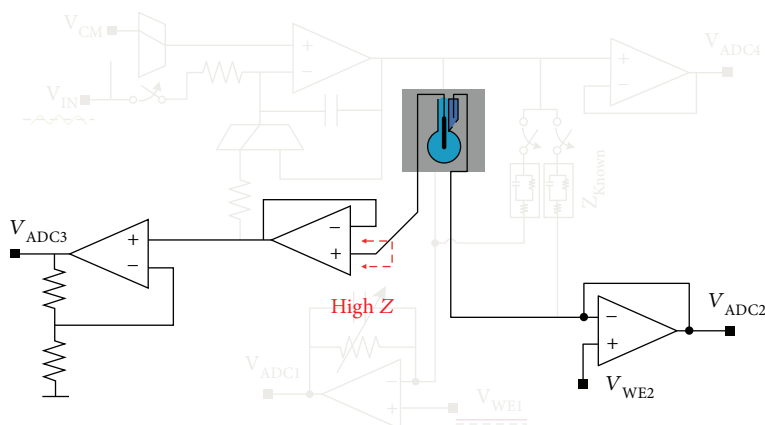


FIGURE 23: Schematic of the potentiostat in potentiometric mode. Reprinted from [34].



FIGURE 24: Block diagram of the biosensor. Reprinted from [59].

with the DC resolution up to  $75 \mu\text{V}$ , whereas some potentiostat units use the R2R ladder circuit to generate the analog waveform for voltammetry [63], whose R2R circuit has some limitations mainly due to the tolerance of the resistance. In this picture, regarding the design of the voltage control of the potentiostat, the most advisable aspect to take into consideration is its ability to be accurate and provide the exact voltage required and at the same time to be easily configurable by the users. Similarly, most of the current values lie in nanoampere and microampere ranges. From the comparison, it can be highlighted that the minimization of the noise in order to detect a small current ( $<100 \text{ pA}$ ) is the most desired features of potentiostat for protein quantification. Indeed, as demonstrated in [31, 32], the possibility to detect such small peaks of current allows reducing the minimum solution concentration, typically in the range of  $\text{ng/ml}$ , and thus improving the clinical relevance of potentiostat use. Another critical issue to take into account in designing a potentiostat is the frequency of the applied stimulus. Among the AC stimulus voltages, [50, 51, 55, 64] employed the largest range of frequency from  $0.1 \text{ Hz}$  to  $100 \text{ kHz}$ , in order to ensure a proper impedimetric configuration. In order to design a highly accurate impedimetric potentiostat, key design considerations are the linearity of the output voltage and the stability of the system in achieving the desired frequency [40]. This is fundamental to precisely control a selected frequency and to sweep over multiple frequencies for proper characterization of the protein.

Regarding the design, the reported studies have focused on the miniaturisation of the electrochemical systems to promote portability [12]. The miniaturisation and portability of these measurement systems are a forwarding step towards accomplishing real-time and fast POC applications to execute rapid in situ analyses [13]. Indeed, measurements or

detection of analytes could be performed in several locations [17], for instance, in a nonhospital setting by unskilled staff or at home by patients, while analyses in laboratories are time-consuming and costly processes.

For POC diagnostic applications, the potentiostat should be easy to use, portable, and self-contained [17] having the capability to interact with biological samples directly and provide real-time information [19]. Cruz et al. [19] also highlighted that miniature analytical devices will be beneficial for the monitoring of physiological parameters and the detection of diseases at early stages at POC. Considering the design, [33] used ADC with maximum resolution of 24 bits and DAC with a maximum resolution of 16 bits to reduce quantization error. Only [28–34] practically designed portable potentiostats that have the potential to be used for POC testing. The programmable, portable, and telemetric biosensor proposed by Jung et al. [65] can be considered a great example of the POC biosensor, but it was designed for detection of a metabolite, ruthenium(III) chloride. However, similar design considerations can be translated for protein detection. Sensitivity and selectivity are important features regarding the functionality of the potentiostats. The discussed potentiostats are highly sensitive, since their minimum current detection range is between  $100 \text{ nA}$  to  $600 \text{ fA}$ , except [34]. Electrochemical biosensors should be tested with different samples containing target and nontarget biomolecules to investigate the sensitivity and selectivity at the time [65]. This will validate the performance of a potentiostat, further validating the practical application of POC potentiostats.

### 3. Conclusion

In this review, we have investigated the design considerations and reported the analysis on measurement characteristics of

TABLE 1: Detailed comparison of the techniques.

Characteristics	Voltammetric/amperometric protein detection	Impedimetric protein detection	Potentiometric protein detection
General working principle	Voltammetry methods measure current as a function of applied potential wherein the polarization of the indicator or working electrode is enhanced	A sinusoidal stimulus current/voltage with a varying frequency is applied over time for which the resultant voltage/current is measured, whose amplitude and phase change provide information related to target molecules	Potentiometry measures the potential of a solution between two electrodes, affecting the solution very little in the process. One electrode is called the reference electrode and has a constant potential, while the other one is an indicator electrode whose potential changes with the composition of the sample. Therefore, the difference of the potential between the two electrodes gives an assessment of the composition of the sample.
Changing/varying parameter	The cell's current is measured while actively altering the cell's potential	The change in resistance and/or capacitance occurs during detection events	The difference in electrode potentials is measured
Governing equation/plot	Nernst or Butler-Volmer equation	Nyquist plot	Nernst equation
Output	They are described as a function of applied potential, measured current, and time	Impedance data	Measures analyte concentration using potential
Sensitivity	High	Moderate to high	Moderate
Other contrasting features	(i) Excellent sensitivity (ii) Simultaneous determination of several analytes (iii) Rapid analysis times	(i) Very small stimulus voltage (ii) Label free nature	Ability to detect free ions
Noise	Gives smooth responses without noise distortion	Impedance drift and noise have been reported at 100 Hz and lower frequencies.	Possesses noise elimination capability

TABLE 2: Technical comparison of the discussed potentiostats.

Author	Year	Protein detected	Voltage	Current	Frequency	Portability	Programmability	Sensitivity
<i>Voltammetric/amperometric protein detection</i>								
Loncatic et al. [28]	2012	Lysozyme	-0.4 V	7.4 nA	—	Portable	Programmable	High
Muid et al. [29]	2014	—	±1.6 mV	—	1 Hz to 1 kHz	Portable	Nonprogrammable	—
Molinari et al. [32]	2015	β-Casein	-0.28 V	2 μA to 0.72 μA	—	Portable	Nonprogrammable	High
Dryden and Wheeler [33]	2015	—	-0.25 V-0.52 V <sup>1</sup> -0.15 V-0.5 V <sup>2</sup> -0.3 V-0.25 V <sup>3</sup>	—	60 Hz <sup>1</sup> 70 Hz <sup>2</sup> 500 Hz <sup>3</sup>	Portable	Nonprogrammable	—
Sun et al. [34]	2016	—	-0.2 V to 0.3 V (lactoferrin) 0.5 V (Glucose)	40 μA to 150 μA 7 μA to 17 μA	—	Portable	Nonprogrammable	—
Cruz et al. [19]	2014	—	±0.6 V	-13 μA to 13 μA	—	Portable	Programmable	—
Ghoreishzadeh et al. [35]	2017	—	0.65 V	0.1 μA to 3 μA	—	Portable	Programmable gain setting Programmable μC driving DAC	—
Medina-Sánchez et al. [39]	2014	Apolipoprotein E	-0.85 V	0.11 μA	25 Hz	Portable	Nonprogrammable	High
<i>Impedimetric protein detection</i>								
Pruna et al. [49]	2018	TNF-α	±2.5 V	—	1-10 Hz	Portable	Programmable	High
Huang et al. [50]	2011	—	10 mV	—	0.1 Hz to 100 kHz	Portable	Nonprogrammable	—
Ogurtsov et al. [51]	2017	—	10 mV	—	10 Hz to 100 kHz	Portable	Programmable gain setting	—
Sun et al. [34]	2016	NeutrAvidin	0.2 V	—	1 Hz to 10 kHz	Portable	Nonprogrammable	Moderate
Esfandyarpour et al. [52]*	2013	Biotin and streptavidin	Vrms of 100 mV	—	1-10 kHz	Nonportable	Programmable for impedance techniques and not for voltammetry	High
Esfandyarpour et al. [53]*	2013	Streptavidin	Vrms of 100 mV	—	15 kHz	Nonportable	Programmable for impedance techniques and not for voltammetry	Moderate
Bellagambi et al. [54]*	2017	TNF-α	0.228 V	—	—	Nonportable	Programmable current and voltage resolution	High
Baraket et al. [55]*	2017	Interleukin-1 and Interleukin-10	0.228 V	—	0.1 Hz-100 kHz	Nonportable	Programmable current and voltage resolution	High
<i>Potentiometric protein detection</i>								
Dryden and Wheeler [33]	2015	—	2.3 mV	—	30 kHz	Portable	Nonprogrammable	—
Huang et al. [57]	2004	—	0 V-5 V	1 μA to 1 mA	—	Portable	Programmable	—
Sun et al. [34]	2016	—	—	—	—	Portable	Nonprogrammable	—
Ma et al. [59]	2016	—	-0.2 to 1 V	—	—	Portable	Nonprogrammable	—

<sup>1</sup>Cyclic voltammetry, <sup>2</sup>squarewave voltammetry, <sup>3</sup>differential pulse voltammetry; \*commercial potentiostats.

TABLE 3: Detailed technical comparison of the discussed proteins.

Author	Supply voltage	Scan rate	Potentiostat operating voltage	ADC bits for I->V	Electrode type	Accuracy	Type of noise	CMOS chip	Communication method	Voltammetry type	Current limitations
<i>Voltammetric/amperometric protein detection</i>											
Loncaric et al. [28]	5 V	10–500 mV/s.	±2.5 V	10 bits	WE—gold CE—platinum RE—Ag/AgCl	Relative uncertainty is <0.6%	Peak-to-peak noise fluctuation 5 nA	No	USB-powered and controlled	Cyclic voltammetry	Current detection limit 15 nA
Muid et al. [29]	5 V	10 mV/s	±1.6 V	12 bits	Commercial Ag/AgCl electrode	Relative error under 2.5%	—	No	USB-powered and controlled	Cyclic, squarewave voltammetry	Minimum detectable current 10 $\mu$ A
Molinari et al. [32]	3.7 V	—	±2.5	10 bits	Commercial Ag/AgCl electrode	—	—	No	Wireless & battery-operated	Cyclic voltammetry	—
Dryden and Wheeler [33]	5 V	100 mV/s	±1.5 V	24 bits	Commercial DropSens electrodes	Small signal error due to higher ADC resolution	Thermal noise, environmental noise	No	USB-powered and controlled	Cyclic, squarewave voltammetry	Minimum detectable current 600 fA
Sun et al. [34]	2.5–5.5 V	25 mV/s	±0.4 V	16 bits	Commercial DropSens electrodes with WE—gold	—	i/p referred current noise, i/p referred voltage noise	No	Wireless (Bluetooth)	Cyclic voltammetry	Detectable current range 800 pA–200 $\mu$ A
Cruz et al. [19]	5 V	50 mV/s	±0.6 V	16 bits	Modified Au-microelectrode (WE)	—	—	No	USB-powered and controlled	Cyclic voltammetry	Minimum current generated 1.24 $\mu$ A/M
Ghoreishzadeh et al. [35]	3.3 V	—	—	10 bits	WE—gold CE—platinum RE—Ag/AgCl CE & WE—graphite The highlighted part is grammatically unclear/incorrect. Please rephrase this part for the sake of clarity and correctness.—Ag/AgCl	High	Input-referred noise of 0.47 pA	Yes CMOS	Wireless (Bluetooth)	Cyclic voltammetry	Detectable current range $\pm 20 \mu$ A
<i>Impedimetric</i>											
Pruna et al. [49]	5 V	100 mV/s	±2.5 V	10 bits	WE—gold CE—platinum RE—Ag/AgCl	Good	Noise due to intrinsic nature of biosensor,	No	Serial communication	Cyclic voltammetry	—
Huang et al. [50]	5 V-	—	±2.5 V	16 bits	CE—platinum RE—Ag/AgCl WE—ITO-coated glass slide	—	White noise, periodic noise	No	USB-powered and controlled	Cyclic voltammetry	—

TABLE 3: Continued.

Author	Supply voltage	Scan rate	Potentiostat operating voltage	ADC bits for I->V	Electrode type	Accuracy	Type of noise	CMOS chip	Communication method	Voltammetry type	Current limitations	
Ogurtsov et al. [51]	5–12 V	100 mV/s	—	12 bits	WE—gold CE—platinum RE—Ag/AgCl	Zero measurement errors	—	No	Serial communication	Cyclic voltammetry	—	
Sun et al. [34]	2.5–5.5 V	25 mV/s	±0.4 V	16 bits	Commercial DropSens electrodes with WE—gold	—	i/p referred current noise, i/p referred voltage noise	No	Wireless (Bluetooth)	Cyclic voltammetry	Detectable current range 800 pA–200 $\mu$ A	
Baraket et al. [55]	5 V	100 mV/s	±2.5 V	—	WE—gold CE—platinum RE—Ag/AgCl	—	—	No	USB-powered and controlled	Cyclic voltammetry	Detectable current range 1 nA–400 mA	
<i>Potentiometric</i>												
Dryden and Wheeler [33]	5 V	100 mV/s	±1.5 V	24 bits	Commercial DropSens electrodes	Small signal error due to higher ADC resolution	Thermal noise, environmental noise	No	USB-powered and controlled	Cyclic, squarewave voltammetry	Minimum detectable current 600 fA	
Huang et al. [57]	5 V	—	—	12 bits	WE—Pt+SLBTLO CE—Pt+Alu RE—Ag/AgCl	Deviation is 1.82% from the commercial potentiostat	—	No	Wirelessly controlled	Cyclic voltammetry	Detectable current range 1 $\mu$ A–1 mA	
Sun et al. [34]	2.5–5.5 V	25 mV/s	±0.4 V	16 bits	Commercial DropSens electrodes with WE—gold	—	i/p referred current noise, i/p referred voltage noise	No	Wireless (Bluetooth)	Cyclic voltammetry	Detectable current range 800 pA–200 $\mu$ A	
Ma et al. [59]	3.7 V	50 mV/s	-0.2 V–1.0 V1	12 bits	WE—gold CE—gold RE—Ag/AgCl	High	Out-of-band noise	No	Wireless (Zigbee)	Cyclic voltammetry	—	

potentiostats specifically used for protein biosensing. Despite that biochemical and immune-assays are still considered the reliable gold standard for protein quantification, they show limitations in terms of time, expertise required, cost, and detection volumes. Therefore, there is an urgent need to develop real-time, portable, highly sensitive, selective, miniaturized, multichannel, and easy-to-use diagnostic tools for early detection of diseases. This review classified the potentiostats into three major categories (potentiometric, impedimetric, and voltammetric) based on the operations and reported their measurement characteristics. Tables 2 and 3 demonstrate how a proper potentiostat for protein characterization should be selected based on the supply voltage typically in the range of mV to few V; also, there is a higher demand of readability of current, typically within the range of some 100 pA, which requires a higher ADC resolution ranging from 10 bits to 24 bits and a sensitivity of detection with variable scan rates ranging from 10 mV/s to 1.2 V/s. Overall, this review summarizes the design considerations for potentiostat and how the research is moving forward in the direction of designing portable, programmable, highly sensitive, miniaturized, and real-time potentiostats, opening the possibility of POC testing without going to the laboratory.

## Conflicts of Interest

The authors declare that they have no conflicts of interest.

## References

- [1] P. Mehrotra, "Biosensors and their applications - a review," *Journal of Oral Biology and Craniofacial Research*, vol. 6, no. 2, pp. 153–159, 2016.
- [2] S. Choi, M. Goryll, L. Y. M. Sin, P. K. Wong, and J. Chae, "Microfluidic-based biosensors toward point-of-care detection of nucleic acids and proteins," *Microfluidics and Nanofluidics*, vol. 10, no. 2, pp. 231–247, 2011.
- [3] D. De Venuto, M. D. Torre, C. Boero, S. Carrara, and G. De Micheli, "A novel multi-working electrode potentiostat for electrochemical detection of metabolites," in *2010 IEEE Sensors*, pp. 1572–1577, Kona, HI, USA, 2010.
- [4] S. Vigneshvar, C. C. Sudhakumari, B. Senthilkumaran, and H. Prakash, "Recent advances in biosensor technology for potential applications—an overview," *Frontiers in Bioengineering and Biotechnology*, vol. 4, p. 11, 2016.
- [5] A. Prasad, K. Mahato, P. K. Maurya, and P. Chandra, "Biomaterials for biosensing applications," *Journal of Analytical & Bioanalytical Techniques*, vol. 7, no. 2, article e124, 2016.
- [6] B. Cai, S. Wang, L. Huang, Y. Ning, Z. Zhang, and G.-J. Zhang, "Ultrasensitive label-free detection of PNA–DNA hybridization by reduced graphene oxide field-effect transistor biosensor," *ACS Nano*, vol. 8, no. 3, pp. 2632–2638, 2014.
- [7] M. M. Barsan, M. E. Ghica, and C. M. A. Brett, "Electrochemical sensors and biosensors based on redox polymer/carbon nanotube modified electrodes: a review," *Analytica Chimica Acta*, vol. 881, pp. 1–23, 2015.
- [8] H. Li, X. Liu, L. Li, X. Mu, R. Genov, and A. Mason, "CMOS electrochemical instrumentation for biosensor microsystems: a review," *Sensors*, vol. 17, no. 12, p. 74, 2017.
- [9] A. Bewick and M. Fleischmann, "The design and performance of potentiostats," *Electrochimica Acta*, vol. 8, no. 3, pp. 89–106, 1963.
- [10] Y.-H. Sheu and C.-Y. Huang, "A portable potentiostat for electrochemical sensors," in *3rd Kuala Lumpur International Conference on Biomedical Engineering 2006*, vol. 15 of *IFMBE Proceedings*, pp. 538–542, Kuala Lumpur, Malaysia, 2006, Springer.
- [11] E. S. Friedman, M. A. Rosenbaum, A. W. Lee, D. A. Lipson, B. R. Land, and L. T. Angenent, "A cost-effective and field-ready potentiostat that poises subsurface electrodes to monitor bacterial respiration," *Biosensors and Bioelectronics*, vol. 32, no. 1, pp. 309–313, 2012.
- [12] L. Oluwole, T. O. Adegoke, and O. O. Ajide, "Development of a field-portable digital potentiostat," *International Journal of Scientific and Engineering Research*, vol. 5, pp. 654–661, 2014.
- [13] J. Colomer-Farrarons, P. L. Miribel-Català, A. I. Rodríguez-Villarreal, and J. Samitier, "Portable bio-devices: design of electrochemical instruments from miniaturized to implantable devices," in *New Perspectives in Biosensors Technology and Applications*, pp. 373–400, InTech, 2011.
- [14] C.-Y. Huang, "Design of a portable potentiostat with dual-microprocessors for electrochemical biosensors," *Universal Journal of Electrical and Electronic Engineering*, vol. 3, no. 6, pp. 159–164, 2015.
- [15] D. Harvey, "Analytical Chemistry 2.0—an open-access digital textbook," *Analytical and Bioanalytical Chemistry*, vol. 399, no. 1, pp. 149–152, 2011.
- [16] Y. Wang, H. Xu, J. Zhang, and G. Li, "Electrochemical sensors for clinic analysis," *Sensors*, vol. 8, no. 4, pp. 2043–2081, 2008.
- [17] A. Nemiroski, D. C. Christodouleas, J. W. Hennek et al., "Universal mobile electrochemical detector designed for use in resource-limited applications," *Proceedings of the National Academy of Sciences*, vol. 111, no. 33, pp. 11984–11989, 2014.
- [18] C. D. García, K. Y. Chumbimuni-Torres, and E. Carrilho, Eds., *Capillary electrophoresis and microchip capillary electrophoresis: principles, applications, and limitations*, John Wiley & Sons, Inc., Hoboken, NJ, USA, 2013.
- [19] A. F. D. Cruz, N. Norena, A. Kaushik, and S. Bhansali, "A low-cost miniaturized potentiostat for point-of-care diagnosis," *Biosensors and Bioelectronics*, vol. 62, pp. 249–254, 2014.
- [20] N. Chaffey, "Alberts, B., Johnson, A., Lewis, J., Raff, M., Roberts, K. and Walter, P. Molecular biology of the cell. 4th edn," *Annals of Botany*, vol. 91, no. 3, pp. 401–401, 2003.
- [21] M. W. Gonzalez and M. G. Kann, "Chapter 4: protein interactions and disease," *PLoS Computational Biology*, vol. 8, no. 12, article e1002819, 2012.
- [22] J. Wang, *Analytical electrochemistry*, Wiley-VCH, 2006.
- [23] P. Bemnowicz, G.-Z. Yang, S. Anastasova, A.-M. Spehar-Deleze, and P. Vadgama, "Wearable electronic sensor for potentiometric and amperometric measurements," in *2013 IEEE International Conference on Body Sensor Networks*, pp. 1–5, Cambridge, MA, USA, 2013.
- [24] J. Punter, J. Colomer-Farrarons, and P. L. Miribel, "Bioelectronics for amperometric biosensors," in *State of the Art in Biosensors-General Aspects*, pp. 241–274, InTech, 2013.
- [25] M. Li, Y.-T. Li, D.-W. Li, and Y.-T. Long, "Recent developments and applications of screen-printed electrodes in environmental assays—a review," *Analytica Chimica Acta*, vol. 734, pp. 31–44, 2012.

- [26] N. Elgrishi, K. J. Rountree, B. D. McCarthy, E. S. Rountree, T. T. Eisenhart, and J. L. Dempsey, "A practical beginner's guide to cyclic voltammetry," *Journal of Chemical Education*, vol. 95, no. 2, pp. 197–206, 2017.
- [27] A. J. Bard and L. R. Faulkner, *Electrochemical Methods: Fundamentals and Applications*, Wiley, 2001.
- [28] C. Loncaric, Y. Tang, C. Ho, M. A. Parameswaran, and H. Z. Yu, "A USB-based electrochemical biosensor prototype for point-of-care diagnosis," *Sensors and Actuators B: Chemical*, vol. 161, no. 1, pp. 908–913, 2012.
- [29] A. Muid, M. Djamal, and R. Wirawan, "Development of a low cost potentiostat using ATXMEGA32," *AIP Conference Proceedings*, vol. 1589, pp. 124–128, 2012.
- [30] K. Kellner, T. Posnicek, J. Ettenauer, K. Zuser, and M. Brandl, "A new, low-cost potentiostat for environmental measurements with an easy-to-use PC interface," *Procedia Engineering*, vol. 120, pp. 956–960, 2015.
- [31] S. Kwakye and A. Baeumner, "An embedded system for portable electrochemical detection," *Sensors and Actuators B: Chemical*, vol. 123, no. 1, pp. 336–343, 2007.
- [32] J. Molinari, C. Moina, and G. Ybarra, "Electrochemical immunosensor for the determination of  $\beta$ -casein," *Journal of Electrochemical Science and Engineering*, vol. 5, no. 1, pp. 9–16, 2015.
- [33] M. D. M. Dryden and A. R. Wheeler, "DStat: a versatile, open-source potentiostat for electroanalysis and integration," *PLoS One*, vol. 10, no. 10, article e0140349, 2015.
- [34] A. Sun, A. G. Venkatesh, and D. A. Hall, "A multi-technique reconfigurable electrochemical biosensor: enabling personal health monitoring in mobile devices," *IEEE Transactions on Biomedical Circuits and Systems*, vol. 10, no. 5, pp. 945–954, 2016.
- [35] S. S. Ghoreishizadeh, I. Taurino, G. De Micheli, S. Carrara, and P. Georgiou, "A differential electrochemical readout ASIC with heterogeneous integration of bio-nano sensors for amperometric sensing," *IEEE Transactions on Biomedical Circuits and Systems*, vol. 11, no. 5, pp. 1148–1159, 2017.
- [36] A. Ainla, M. P. S. Mousavi, M. N. Tsaloglou et al., "Open-source potentiostat for wireless electrochemical detection with smartphones," *Analytical Chemistry*, vol. 90, no. 10, pp. 6240–6246, 2018.
- [37] G. F. Giordano, M. B. R. Vicentini, R. C. Murer et al., "Point-of-use electroanalytical platform based on homemade potentiostat and smartphone for multivariate data processing," *Electrochimica Acta*, vol. 219, pp. 170–177, 2016.
- [38] M. D. Steinberg, P. Kassal, I. Kereković, and I. M. Steinberg, "A wireless potentiostat for mobile chemical sensing and biosensing," *Talanta*, vol. 143, pp. 178–183, 2015.
- [39] M. Medina-Sánchez, S. Miserere, E. Morales-Narváez, and A. Merkoçi, "On-chip magneto-immunoassay for Alzheimer's biomarker electrochemical detection by using quantum dots as labels," *Biosensors and Bioelectronics*, vol. 54, pp. 279–284, 2014.
- [40] E. B. Bahadır and M. K. Sezginürk, "A review on impedimetric biosensors," *Artificial Cells, Nanomedicine, and Biotechnology*, vol. 44, no. 1, pp. 248–262, 2016.
- [41] J.-G. Guan, Y.-Q. Miao, and Q.-J. Zhang, "Impedimetric biosensors," *Journal of Bioscience and Bioengineering*, vol. 97, no. 4, pp. 219–226, 2004.
- [42] F. Lisdat and D. Schäfer, "The use of electrochemical impedance spectroscopy for biosensing," *Analytical and Bioanalytical Chemistry*, vol. 391, no. 5, pp. 1555–1567, 2008.
- [43] B.-Y. Chang and S.-M. Park, "Electrochemical impedance spectroscopy," *Annual Review of Analytical Chemistry*, vol. 3, no. 1, pp. 207–229, 2010.
- [44] S. Petrovic, "Cyclic voltammetry of hexachloroiridate(IV): an alternative to the electrochemical study of the ferricyanide ion," *The Chemical Educator*, vol. 5, no. 5, pp. 231–235, 2000.
- [45] S.-M. Park and J.-S. Yoo, "Electrochemical impedance spectroscopy for better electrochemical measurements," *Analytical Chemistry*, vol. 75, no. 21, pp. 455A–461A, 2003.
- [46] J. S. Daniels and N. Pourmand, "Label-free impedance biosensors: opportunities and challenges," *Electroanalysis*, vol. 19, no. 12, pp. 1239–1257, 2007.
- [47] M. Citartan, S. C. B. Gopinath, J. Tominaga, and T. H. Tang, "Label-free methods of reporting biomolecular interactions by optical biosensors," *Analyst*, vol. 138, no. 13, pp. 3576–3592, 2013.
- [48] S. Sang, Y. Wang, Q. Feng, Y. Wei, J. Ji, and W. Zhang, "Progress of new label-free techniques for biosensors: a review," *Critical Reviews in Biotechnology*, vol. 36, no. 3, pp. 465–481, 2016.
- [49] R. Pruna, F. Palacio, A. Baraket et al., "A low-cost and miniaturized potentiostat for sensing of biomolecular species such as TNF- $\alpha$  by electrochemical impedance spectroscopy," *Biosensors and Bioelectronics*, vol. 100, pp. 533–540, 2018.
- [50] X. Huang, H. Chen, H. Deng, L. Wang, S. Liao, and A. Tang, "A fast and simple electrochemical impedance spectroscopy measurement technique and its application in portable, low-cost instrument for impedimetric biosensing," *Journal of Electroanalytical Chemistry*, vol. 657, no. 1–2, pp. 158–163, 2011.
- [51] V. I. Ogurtsov, K. Twomey, and J. Pulka, "A portable sensing system for impedance based detection of biotoxin substances," in *Proceedings of the 10th International Joint Conference on Biomedical Engineering Systems and Technologies (BIOSTEC 2017)*, pp. 54–62, Porto, Portugal, 2017.
- [52] R. Esfandyarpour, H. Esfandyarpour, M. Javanmard, J. S. Harris, and R. W. Davis, "Microneedle biosensor: a method for direct label-free real time protein detection," *Sensors and Actuators B: Chemical*, vol. 177, pp. 848–855, 2013.
- [53] R. Esfandyarpour, M. Javanmard, Z. Koochak, H. Esfandyarpour, J. S. Harris, and R. W. Davis, "Thin film nanoelectronic probe for protein detection," *MRS Proceedings*, vol. 1572, 2013.
- [54] F. G. Bellagambi, A. Baraket, A. Longo et al., "Electrochemical biosensor platform for TNF- $\alpha$  cytokines detection in both artificial and human saliva: heart failure," *Sensors and Actuators B: Chemical*, vol. 251, pp. 1026–1033, 2017.
- [55] A. Baraket, M. Lee, N. Zine, M. Sigaud, J. Bausells, and A. Errachid, "A fully integrated electrochemical biosensor platform fabrication process for cytokines detection," *Biosensors and Bioelectronics*, vol. 93, pp. 170–175, 2017.
- [56] A. Das, P. Bhadri, F. R. Beyette, A. Jang, P. Bishop, and W. Timmons, "A potentiometric sensor system with integrated circuitry for in situ environmental monitoring," in *2006 Sixth IEEE Conference on Nanotechnology*, pp. 917–920, Cincinnati, OH, USA, 2006.
- [57] C. Y. Huang, H. Y. Lin, Y. C. Wang, W. Y. Liao, and T. C. Chou, "A portable and wireless data transmission potentiostat," in *The 2004 IEEE Asia-Pacific Conference on Circuits and Systems*, pp. 633–636, Tainan, Taiwan, 2004.

- [58] C. Berggren, B. Bjarnason, and G. Johansson, "An immunological interleukine-6 capacitive biosensor using perturbation with a potentiostatic step," *Biosensors and Bioelectronics*, vol. 13, no. 10, pp. 1061–1068, 1998.
- [59] W. J. Ma, C. H. Luo, J. L. Lin et al., "A portable low-power acquisition system with a urease bioelectrochemical sensor for potentiometric detection of urea concentrations," *Sensors*, vol. 16, no. 4, 2016.
- [60] B. J. Privett, J. H. Shin, and M. H. Schoenfisch, "Electrochemical sensors," *Analytical Chemistry*, vol. 80, no. 12, pp. 4499–4517, 2008.
- [61] F. J. Gruhl, B. E. Rapp, and K. Länge, *Biosensors for Diagnostic Applications*, Springer, Berlin, Heidelberg, 2011.
- [62] S. Tonello, G. Abate, M. Borghetti et al., "Wireless point-of-care platform with screen-printed sensors for biomarkers detection," *IEEE Transactions on Instrumentation and Measurement*, vol. 66, no. 9, pp. 2448–2455, 2017.
- [63] B. Aremo, M. Oyebamiji Adeoye, I. B. Obioh, and O. A. Adeboye, "A simplified microcontroller based potentiostat for low-resource applications," *Open Journal of Metal*, vol. 5, no. 4, pp. 37–46, 2015.
- [64] C.-Y. Huang, Y.-C. Wang, H.-C. Chen, and K.-C. Ho, "Design of a portable potentiostat for electrochemical sensors," in *Proceedings of the 2004 Intelligent Sensors, Sensor Networks and Information Processing Conference, 2004*, pp. 331–336, Melbourne, VIC, Australia, 2004.
- [65] J. Jung, J. Lee, S. Shin, and Y. Kim, "Development of a telemetric, miniaturized electrochemical amperometric analyzer," *Sensors*, vol. 17, no. 10, 2017.

